Some Problems of Seismic Data Processing. Part 2. Data Processing Techniques for the Detection and Analysis of P and S Waves of Local Earthquakes

AUTHOR(S):

FURUZAWA, Tamotsu

CITATION:

FURUZAWA, Tamotsu. Some Problems of Seismic Data Processing. Part 2. Data Processing Techniques for the Detection and Analysis of P and S Waves of Local Earthquakes. Bulletin of the Disaster Prevention Research Institute 1974, 24(3): 127-145

ISSUE DATE:

1974-09

URL:

http://hdl.handle.net/2433/124846

Some Problems of Seismic Data Processing

Part 2. Data Processing Techniques for the Detection and Analysis of P and S Waves of Local Earthquakes

By Tamotsu FURUZAWA

(Manuscript received October 1, 1974)

Abstract

The automated-analysis system for P and S waves of the local earthquakes obtained by the short-period system set up at the Amagase Crustal Movement Observatory are described. Firstly, as the basic knowledges necessary for automated analysis, the nature of noise, the frequency characteristics of P and S waves and the nature of particle motions are described. The system is composed of the determination of P onset, the determination of the directions of arrival and incidence of P waves, the determination of onsets of SH and SV waves and the computations of spectra of P, SH and SV waves. Onsets of P and S waves are determined by utilizing changes of both amplitude level and frequency between noise and signal. In the present method, it may be possible to determine the onset time of P wave with accuracy of ± 0.05 sec for 90 % of local earthquakes with magnitude above 1.0. As for S wave, the onset time can be determined with accuracy of ± 0.2 sec for about 90 % of events of which the P onset time is defined.

1. Introduction

In Part I[1], the seismic data acquisition system, which has been set up at our laboratory, was reviewed as the first step for establishment of such a seismic data processing system as unifying observational procedure, several analytical and interpretative procedures of seismic signals. The following step of research is to refine the procedure of automated analysis adequate to data obtained from this observational system. To analyse a great deal of digital data, in particular, it is indispensable to develop a new analytical method based on the traditional way.

According to Keilis-Borok's opinion[2], the analysis and interpretation procedures are divided into the four consecutive stages, as follows:

I) Detection of signal in background noise, measurement of parameters such as arrival time, amplitude, apparent period, and so on, and preliminary identification of signals.

II) Determination of source parameters and refined identification of signals by joint analysis of the data of stage I from many stations.

III) Seismic wave kinematics and dynamics and statistical relations in seismicity.

IV) Seismological interpretations; the earth's structure, earthquake physics and source identification.

Stage II~IV of these four stages have been recently fairly developed as the current subjects of modern seismology with popular use of electronic computers[3]. But the operations in stage I, which recognize the initial information from observed records,

have been little developed, and the practical procedure has been almost carried out manually, which are tedious and lengthy. Therefore, stage I causes a bottleneck in handling a great deal of seismic data. The existence of this bottle neck between the observational procedure and the analytical procedure after stage II checks the entire development of whole system.

Generally it is not yet easy to solve these problems, since much seismological information such as the site characteristics, the nature of various seismic waves and the earth's structure are requisite. In this paper, a particular case will be considered in detail, that is, the method of detection and analysis of P and S initial motions for the local earthquakes obtained by the short-period system settled at Amagase site where the vibrational character has been well known. To find a reliable method of automated identification of P initial phase will be important not only for the seismic analysis but also for the automatic control of the observational systems suitable to lessen the various tedious procedures.

2. Characteristics of Seismic Wave Motion at Amagase Site

A detection of seismic signal by an automatic computer-controller is necessarily based on some knowledges of nature of signals and background noise at a given site. To detect and identify the onset of P or S wave, the effective procedure to discriminate P, S and noise must be carried out by reasonably utilizing their natures. Consequently, the characteristics of background noise, the frequency characteristics of P and S waves and the nature of particle motions concerned with short-period records obtained at Amagase site should be firstly examined.

2.1 Noise Characteristics

Generally speaking, the level of short-period seismic noise at Amagase is relatively

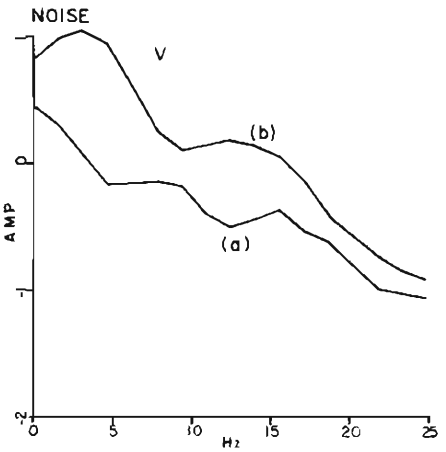

Fig. 1. Amplitude spectra of vertical component for background noise. (a) for an ordinary day, (b) for an extraordinary day when the floodgate of the Amagase dam is opened.

low excepting the extraordinary case induced by water-discharge of the Amagase dam, which is 500 m from the observing site. Noise level of the vertical component is particularly low in the higher frequency range above 5 Hz. And it is not beyond 10 μkine in the predominant frequency range of 0.3 to 0.5 Hz. Fig. 1 illustrates the spectral distributions of background noise of the vertical component, (a) for an ordinary day and (b) the extraordinary case in opening the floodgate of the dam. The level of seismic noise associated with water-discharge is appreciably high in the range from 2 to 3 Hz, and 8~10 times as large as in normal condition. But at high-frequency range the difference in amplitude between both cases is not so much. As seen in Fig. 1(b), the spectral amplitude drops appreciably at frequencies above 5 Hz as compared with below 5 Hz. Though there are such significant differences

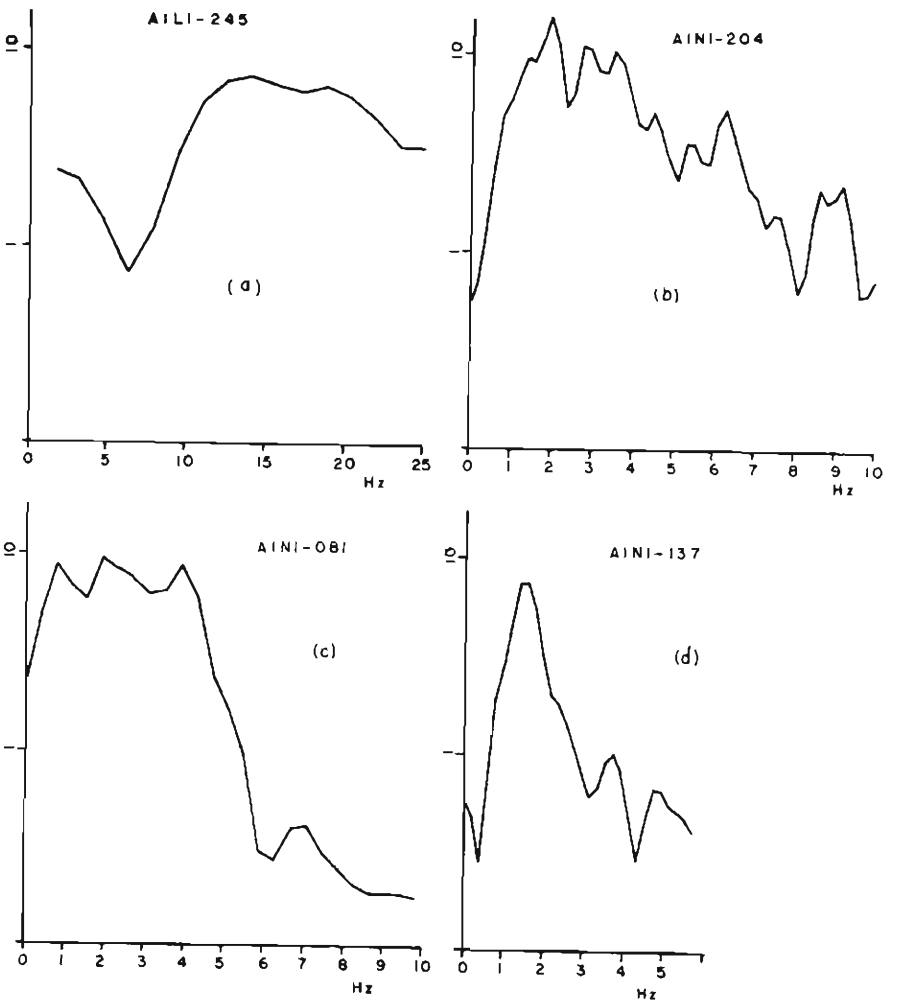

Fig. 2. Amplitude spectra of vertical component of P wave initial parts for events from various epicentral distances;
(a) $\Delta < 20$ km, (b) $\Delta \approx 100$ km, (c) $\Delta \approx 500$ km, (d) $\Delta \approx 1{,}000$ km.

in both shape and level of spectral distribution between noisy and quiet days, the noise characteristics in each case at Amagase is thought to be stationary.

2.2 Frequency Characteristics of P and S Waves

The spectra of body waves should be uniform over the broad frequency band, if signals are emitted as an impulsive form at the source. In practice, however, they have several peaks and troughs due to the various effects of source, propagating path, site condition and so on. Fig. 2 shows the vertical spectra of initial parts of P waves, the epicentral distances which are as follows; (a) $\Delta<20$ km, (b) $\Delta\approx 100$ km, (c) $\Delta\approx 500$ km, and (d) $\Delta\approx 1{,}000$ km, respectively. The peak frequency of spectra lessens with increase of epicentral distance due to the attenuation of high frequency components. For the events of the epicentral distance beyond 500 km, the peak frequencies of spectra are similar to that of noise spectra. On the contrary, the spectra of local earthquakes ($\Delta<20$ km) have a gentle maximum around 15 Hz and generally keep a relatively uniform level at the high-frequency range from 10 to 25 Hz in contrast with noise spectra. Though these peaks and troughs are considerably complicated, the trough of vertical component around 6~8 Hz is commonly recognized through all local earthquakes. For radial component, the trough covers between 3 and 6 Hz and is not so obvious as the vertical component. This trough may correspond to a reverberation effect between the free surface and the observational site at depth of 140 m[4] (shown by site-3 in Fig. 3).

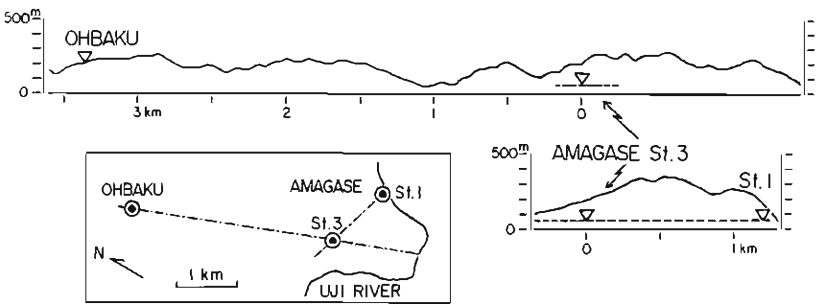

Fig. 3. Topography map of observational stations.

The spectra of S waves for local earthquakes are generally characterized by a uniform level over the broader frequency ranges as compared with those of P waves.

2.3 Particle Motions

As the effective approaches to discriminate seimic signals from a noise background, and in order to identify some phases of interest when three component seismograms at one site are available, the differences in polarization characters of the various kinds of signal and noise are utilized. Since the particle motions are strongly affected by the geological structure, the lateral inhomogeneity and the topography around the observing site, the character of particle motions at a given site must be carefully examined.

Concerning the properties of particle motions of the local earthquakes recorded at Amagase, the following facts have been found[5]: (1) In ordinal condition, the particle motion of background noise is not polarized unidirectionally. (2) The ground noises caused by water-discharge of the dam are transferred as compressional waves, and polarized in the direction connecting the dam with observing site. (3) The polarization of P initial motions originating from local quarry blasts near Amagase

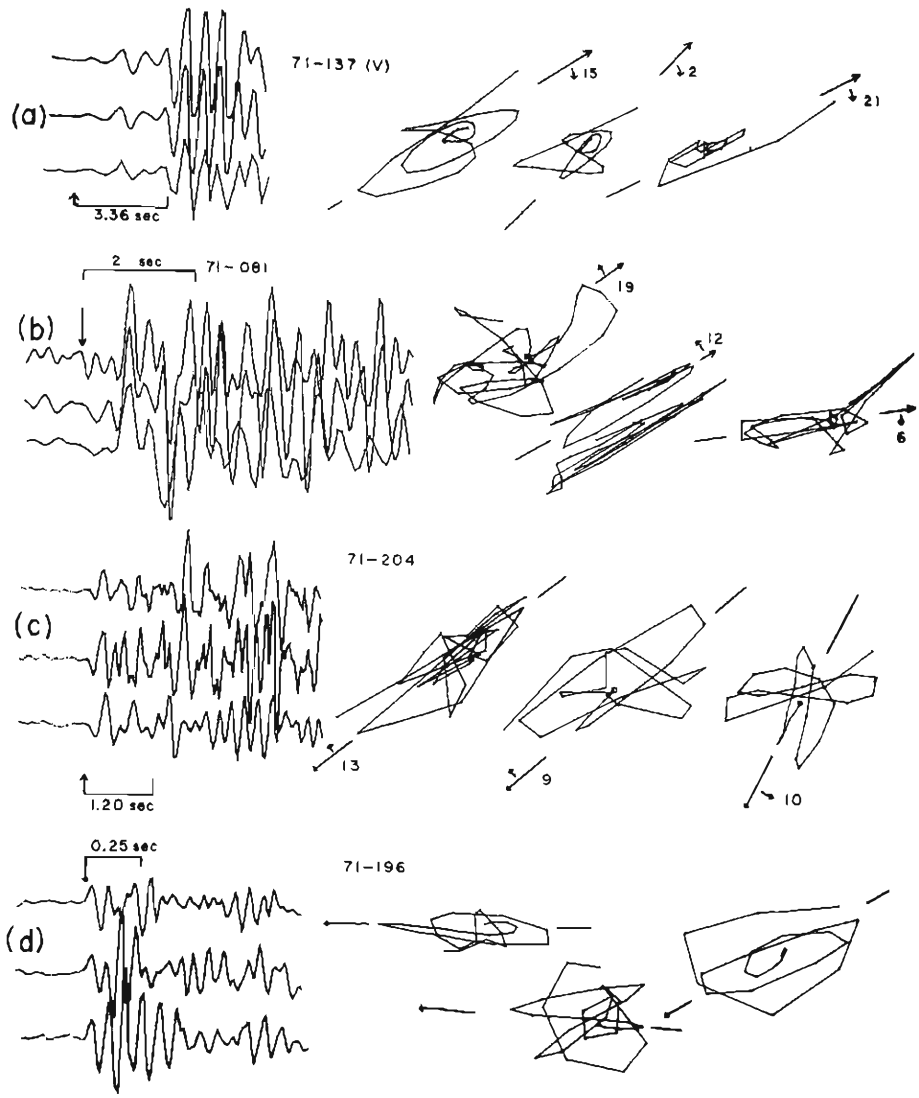

Fig. 4. The vertical waveforms and the particle motions in horizontal plane of P initial parts obtained at three sites;
(a) $\Delta \approx 1{,}000$ km, (b) $\Delta \approx 500$ km, (c) $\Delta \approx 100$ km, (d) $\Delta < 20$ km.
Top trace of waveforms and left side of particle motions: Amagase site-3, middle trace and middle particle motion: Amagase site-1, lowest trace and rightside motion: Ohbaku.

(Δ=1~9 km) directs to the source with an accuracy of about 1~2°, and also the rectilinearity is very clear during the first 1 or 1.5 cycles. (4) For local earthquakes with S-P time below 5 sec, although the rectilinearity is very clear as found in the case of quarry blasts, the westward deflection of P arrival is apparent. The directions of particle motions of S waves are nearly orthogonal with that of P.

Subsequently, to examine the effect of site condition on the surface earthquake motion, the records for the same event obtained at three sites are compared. Three sites consist of Amagase site-3, site-1 set up near the end of the observational gallery, and Ohbaku at about 3.5 km north from Amagase. In Fig. 4 the vertical waveforms of P initial parts and the particle motions in horizontal plane from four events with different epicentral distances are shown. These waves are passed through the low-pass filter with a cut-off frequency corresponded with each peak frequency, since the peak frequency lessens with increase of epicentral distance. As for P waves from a far earthquake with an epicentral distance of about 1,000 km (Fig. 4(a)), due to high attenuation for frequencies above 2 Hz, the mutual accordance of waveforms at the three sites is very high and also the polarizations of particle motions can be clearly determined, permiting somewhat specified deflections to the source direction. In the case of earthquakes of which the epicentral distance is almost 500 km (Fig. 4(b)), the peak frequencies are 3~5 Hz, and these vertical waveforms are rather similar to each other. But the rectilinearity of particle motions for Amagase site-3 is poor, and it is difficult to determine the direction, because the horizontal weveforms in the range of these frequencies are contaminated by some reverberation effects between the free surface and the site located in the gallery at depth of 140 m from ground surface. In the case of near earthquakes of which the peak frequencies are about 15 Hz, on the contrary, the rectilinearity of particle motions at site-3 is remarkable. And moreover, there are not any prominent phases just after the first arrival in comparison with those of the other two sites. At Ohbaku site situated on exposed rock of a mountain ridge, it is difficult to obtain the direction of P arrival of local earthquakes from the waveforms, since particle motions are polarized irregularly.

3 Automated Method of Analysis of P and S Waves

3.1 Detection of P Initial Motion

One of the effective methods for the discrimination of P waves from a background noise is the application of correlation technique, especially suitable for array setting. This technique has been already practically used, and is considerably reliable[6]. This technique enhances some signals and cancels the noise statistically assuming random noise. Therefore, a suitable site for an array is limited by various stringent requirements such as the geological and topographical conditions of the site, the seismic noise level and so on.

In the present case, the deformation of a wave of P initial motions for an event occurring at a distance beyond 500 km is not remarked when the distance of mutual

observational sites is within a few kilometers. Arrays spaced over a distance of a few kilometers are available to record signals at ranges up to about 1,000 km. Therefore, in this case the use of array data is practicable. However, in the case of a local earthquake, the peak frequency of which is higher than 10 Hz, the use of array data is unfavorable because of the poor identification of waveform for pratical analysis, and thus the use of three component data obtained at one site is the only way for the desired purpose. In such case, that is, to determine P initial phase from data obtained at a single site, the traditional method of "eye-reading" has been applied as the only reliable way, but could not prevent the intrinsic obscurity, even with considerable training. Therefore, a method to set a definite amplitude level to control the observational system has been used[1,7]. In this method the P arrival is identified when the amplitude exceeds the stationary noise level at a given site. This method is sometimes affected by the sudden occurence of an abnormal noise and the change of noise level. And thus the threshold must be set up to a somewhat higher level than the usual noise level, but as a result there is fear of missing some signals from weak events.

Generally, when the human eye is used to identify the arrival of P waves, a meaningful difference of frequencies between noise and P wave together with a change of amplitude will be noticed as a useful condition for detection. In the present automated processing system, both the amplitude level and the frequency are utilized. For the character of vertical spectra of local earthquakes obtained at Amagase, as described in 2, there are remarkable differences between the noise part and the P wave part. That is, the level of noise spectra is high in the low frequencies and low beyond 10 Hz. On the other hand, the spectra of P part show their peaks within the range of 10 to 20 Hz. Consequently, if amplitude levels and peak frequencies of the time-dependent spectra of vertical component obtained over the moving time windows of a given length are examined, an interval including P initial part may be discernible due to both the difference of amplitude level and the dissimilarity of spectral shape between noise part and P wave part. This method means to compare the amplitude levels of any two intervals with each other for a certain frequency range. The sensitivity of this method to P initial motion is dependent on the length and the time lag of window used for computation of spectra and moreover on the method of comparision as well. It is desirable to average the noise spectra over wide ranges so that the effect of transient noise becomes as small as possible. To lessen the error due to any deflection of stationarity, the comparison of spectra should be carried out for window being as close as possible.

For the present computation of spectra, the length of 0.64 sec and the time lag of 0.16 sec (1/4 intervals of window) are chosen. The comparison is made by computing the ratio of the spectrum over a given window to the averaged spectrum over the preceding three successive windows. Since the character of noise spectra is stationary in time, the ratio of spectra in the noise interval remains about 1.0 for all frequency ranges. But it becomes larger than 1.0 in the interval including P initial motions. Furthermore, the curve of this ratio versus frequency shows

the slope lifted to the right because of increase of S/N ratio at a higher frequency range than 10 Hz.

Subsequently, the amplitude levels over the interval including P initial part obtained by such a way are examined to determine the onset time of P wave. Firstly, to enhance the S/N ratio and for convenience of analysis of particle motion at a later stage, the three component data in this interval are divided through digital band-pass filters into the following four bands; 5 to 10, 10 to 15, 15 to 20 and 20 to 25 Hz. The signal, passed through each band-pass filter, is reformed into "the instantaneous vector amplitude" in the planes composed of every pair of three components, and then averaged over one cycle at the center frequency of each band. These averaged vector amplitudes as a function of time are compared with the noise amplitude, as defined by the similar way in the noise interval. And the time when the difference of these amplitudes exceeds a given threshold level at two or more bands is defined as the onset of P wave.

3.2 Direction and Rectilinearity of Particle Motion of P Initial Motion

On defining the P initial motion as above described, the arrival direction, the apparent angle of incidence and the rectilinearity are evaluated based on analysis of particle motion. Firstly, the arrival direction of P wave is determined, and then the horizontal components are divided into radial and transverse components by using this value. The arrival direction of P wave is derived from the orientation of the long axis of the elliptical orbit[8], which is drawn in the horizontal plane by wave motion per one cycle of the central frequency of each band. The apparent angle of incidence is obtained in similar fashion for the vertical plane, and the rectilinearity is represented by a normalized correlation coefficient[9] between every two components in each frequency band. Moreover, the duration of P initial motion is defined as the interval where the rectilinearity is remarkable in the vertical plane.

3.3 Ditection of S Initial Motion

The arrival of S wave of a near earthquake is usually contaminated by the coda portion of P wave. This makes the identification of the onset of S wave difficult, so that only a few earthquakes are capable for us to identify precisely as the onset of S wave. This is one of the reasons why S wave arrival has been not discussed in detail for local earthquakes in spite of the importance of S wave analysis in solving the problem of source mechanism.

In the present paper, the S wave onset is identified based on the orthogonal relation of orbital directions of P, SV and SH. As the first step the interval including S initial motion is detected in the same way as P waves. In this case the differences of natures between P and S waves from local earthquakes at Amagase are used. That is, S wave spectra are more predominant at lower frequencies than P and have considerably large amplitude in horizontal components. Moreover, there are no remarkable phases between P and S waves. The directions of particle motion

of S waves are almost orthogonal to the P direction. Therefore, to separate the interval including S initial motion from the coda part of P wave, the time-dependent spectra over the window of 0.64 sec from the transverse component are compared successively in the same way as P wave detection.

And then the waves in this interval are divided into the four bands, which are composed of 2 to 5, 5 to 10, 10 to 15 and 15 to 20 Hz. The onset time of SH arrival is defined as the point where the amplitudes averaged for one cycle of center frequecy of each band exceed the averaged noise in two or more bands. Here, the

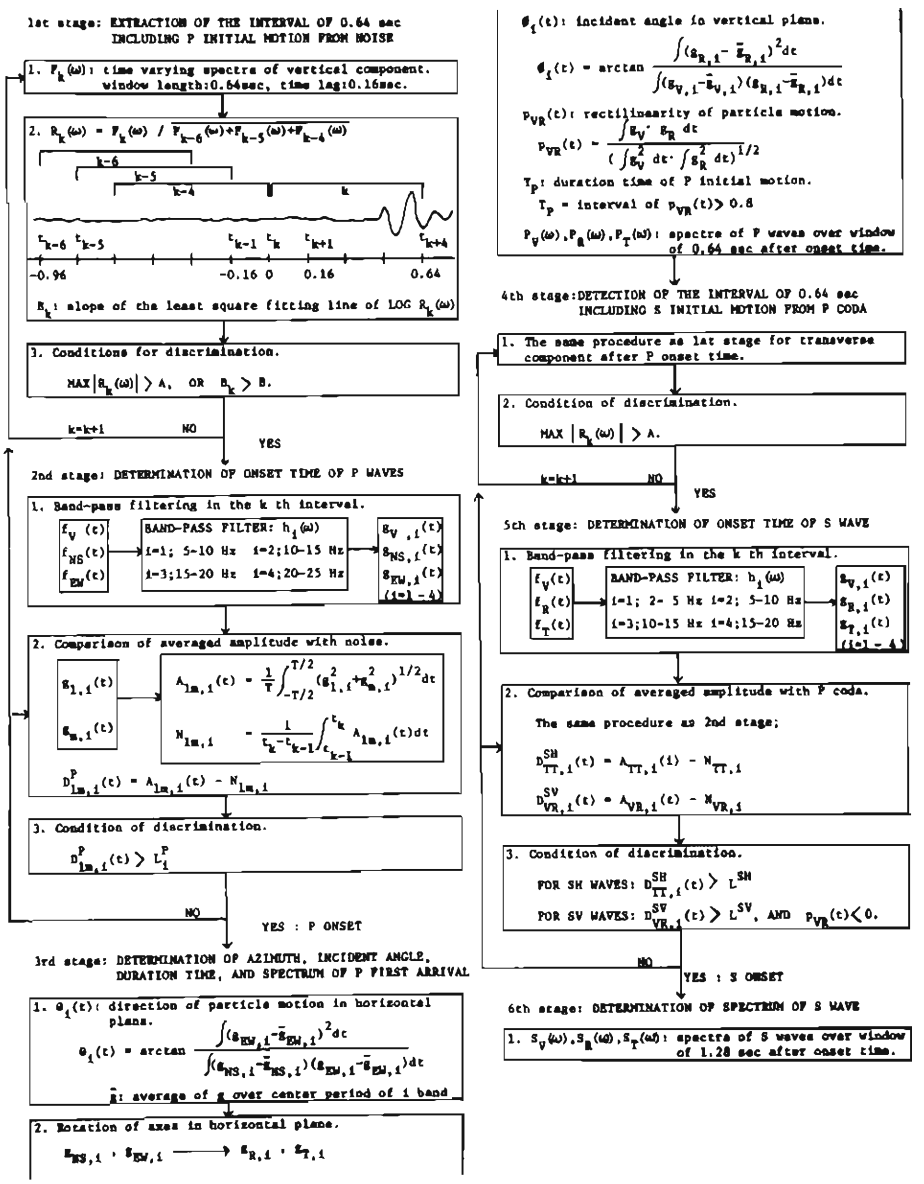

Fig. 5. Flow diagram of the automated analysis system.

noise means P coda parts before S arrival. In SV waves the point where the averaged amplitude in the vertical plane obtained in the same interval as SH waves exceeds the averaged noise level, and furthermore, where the direction of the particle motion becomes orthogonal with P wave, is regarded as the onset time.

3.4 Spectra of P and S Waves

As the final stage of automated analysis, spectra of P, SV and SH waves are computed over the time window, the operation of which starts at the onset time obtained by the procedures above described, with the length of 0.64 sec (P) or 1.28 sec (S).

3.5 Flow Diagram of Automated Analysis System

In Fig. 5 the flow diagram of automated analysis system operated at Amagase is illustrated as the schematic diagram of the methods described above. As the conditions of discriminating P and S waves, the following values have been applied.

The 1st stage: Extraction of the interval of 0.64 sec including P initial motion from noise background.

Ratio of spectrum of the k th interval beginning at a reference time t_k, $F_k(\omega)$, to averaged spectrum over the preceding three successive intervals, of which the entire length is 0.96 sec, beginning at time t_{k-6} and ending at time t_k, and with no overlapping to the k th interval, $\overline{F_{k-6}(\omega)+F_{k-5}(\omega)+F_{k-4}(\omega)}$: $R_k(\omega)$.

Slope of the best fitting line of $\log R_k(\omega)$ in the least square meaning: B_k.

1. MAX$|R_k(\omega)|>4.0$,
2. $B_k>2.5$,
3. MAX$|R_k(\omega)|>2.0$ AND $B_k>1.6$.

If one of these three conditions is satisfied, YES.

The 2nd stage: Determination of onset time of P waves.

The time-dependent amplitudes, in (l, m) plane, averaged over the length equal to one cycle of the center frequency of i th band in the interval determined by 1st stage:

$$A_{lm,i}(t)=\frac{1}{T}\Sigma(g_{l,i}^2(t)+g_{m,i}^2(t))^{1/2}.$$

The similar, averaged amplitude in noise interval:

$$N_{lm,i}=\frac{1}{t_k-t_{k-1}}\Sigma A_{lm,i}(t).$$

The difference between $A_{lm,i}(t)$ and $N_{lm,i}$: $D_{lm,i}{}^P(t)$.

If $D_{lm,i}{}^P(t)$ exceeds the following threshold level, $L_i{}^P$, in two or more adjacent bands, YES.

$$L_1{}^P=3.0\,\mu \text{ kine } (5\sim10\,\text{Hz}),\quad L_2{}^P=2.3\,\mu \text{ kine } (10\sim15\,\text{Hz}),$$
$$L_3{}^P=1.7\,\mu \text{ kine } (15\sim20\,\text{Hz}),\quad L_4{}^P=1.3\,\mu \text{ kine } (20\sim25\,\text{Hz}).$$

The 3rd stage: Determination of azimuth, incident angle and duration of P initial motion.

The time-dependent direction of particle motion of i th band in the horizontal plane per one cycle of the central frequency of band:

$$\theta_i(t)=\arctan\frac{\Sigma(g_{EW,i}(t)-\bar{g}_{EW,i}(t))^2}{\Sigma(g_{NS,i}(t)-\bar{g}_{NS,i}(t))(g_{EW,i}(t)-\bar{g}_{EW,i}(t))},$$

where, $\bar{g}_i$ means an averaged value of band-passed data g_i over one cycle of the center frequency of band, and three bands composed of 5~10, 10~15 and 15~20 Hz are used. $\theta_i(t)$ are computed over the interval of length 0.16 sec, beginning at onset time of P wave, with a sampling interval 0.01 sec. That is, the sixteen values of $\theta_i(t)$ are evaluated in each band. And then the frequency distribution of these 48 quantities is plotted versus every 5° interval, and the maximum frequency value is taken as the arrival direction of P wave.

The apparent angle of incidence is obtained in similar fashion for the time-dependent direction of particle motion in the vertical plane:

$$\phi_i(t)=\arctan\frac{\Sigma(g_{R,i}(t)-\bar{g}_{R,i}(t))^2}{\Sigma(g_{V,i}(t)-\bar{g}_{V,i}(t))(g_{R,i}(t)-\bar{g}_{R,i}(t))}.$$

The normalized correlation coefficient between vertical and radial components which represents the rectilinearity of particle motion in i-th band:

$$p_{VR,i}(t)=\frac{\Sigma g_{V,i}(t)\cdot g_{R,i}(t)}{(\Sigma g_{V,i}^2(t)\cdot\Sigma g_{R,i}^2(t))^{1/2}}.$$

The duration of P initial motion, T_P, is defined as the interval of $p_{VR}(t)\geq 0.8$ in the band of peak frequency of P spectra.

The 4th stage: Extraction of the interval of 0.64 sec including S initial motion from P coda parts.

If $\mathrm{MAX}|R_k(\omega)|>4.0$, YES.

$R_k(\omega)$: spectra ratio for transverse component obtained by the same procedure as the 1st stage.

The 5th stage: Determination of onset time of S wave.

For SH wave, if $D_{TT,i}^{SH}(t)$ exceeds the threshold level, 7.3 μ kine, in two or more adjacent bands within the limit of 0.05 sec, YES.

For SV wave, if $D_{VR,i}^{SV}(t)$ exceeds the threshold level, 6.7 μ kine, in two or more adjacent bands within the limit of 0.05 sec, and if $p_{VR,i}(t)<0$, YES.

Where, $D_{TT,i}^{SH}(t)$ and $D_{VR,i}^{SV}(t)$ are obtained by the same procedure as the 2nd stage and $p_{VR,i}(t)$ the 3rd stage.

4. Results

The duration of 0.64 sec including P first arrival can be best fitted for almost all local earthquakes recorded at Amagase with the magnitude$\geq$1.0. Fig. 6 shows the waveforms composed of three components around P initial parts, the spectra of the noise interval and of the interval including P first arrival, and the ratio of both spectra. Though this figure shows an example for the case where the S/N ratio is very low due to the contamination of noise caused by discharging from the Amagase dam, it shows a successful result in that P first arrival lies in the interval

between P_A and P_B determined by the first stage procedure.

In the next, the reliability of onset time of P wave determined from the second stage is examined. Fig. 7(a) shows the histogram of the differences between the

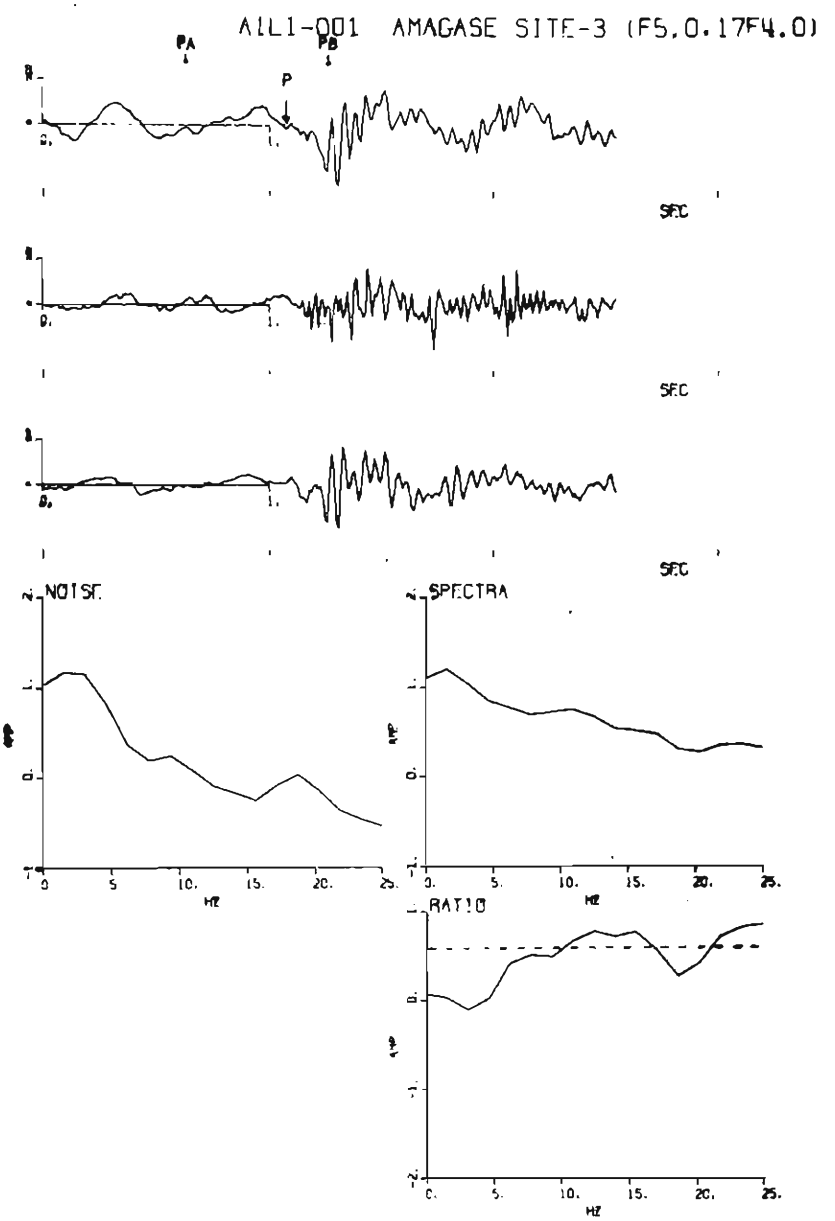

Fig. 6. Three component waveforms around P first arrival, vertical spectra over noise interval and over interval (P_A, P_B), and ratio of those spectra. The interval between P_A and P_B is 0.64 sec including P initial motion determined from 1st stage. P shows onset of P wave. Dotted line of ratio means threshold line of 4.0.

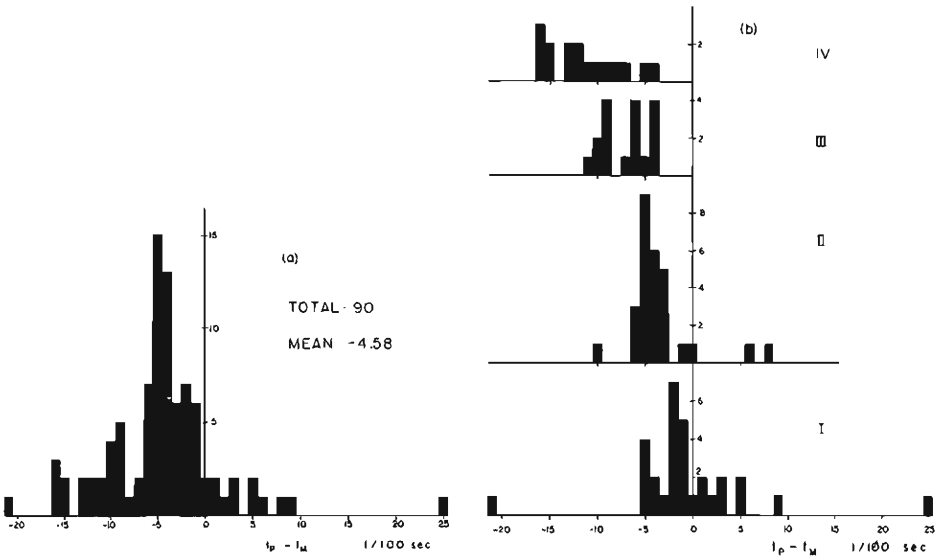

(a) (b)

Fig. 7(a). Histogram of the differences between the P onset time determined from automated method, t_P, and the P onset time read visually, t_M.

Fig. 7(b). Histogram of $t_P - t_M$ classified by the amplitude, A, of P initial motion; I: A<50 digital unit (17 μ kine), II: 50<A<100, III: 100<A<200, IV: A<200.

P onset time determined from automated method, t_P, and the P onset time read visually, t_M, by every 0.01 sec about 90 earthquakes. Though the differences extend from -0.20 sec to $+0.25$ sec, most of these concentrate around -0.05 sec. The present setting, as described in 3.5, is given so as the idenification could be applicable to as many earthquakes of small magnitude as possible, while the effect of side lobe of band-pass filter is not taken into consideration. Therefore, the obtained arrival time is concluded to be earlier than the time read visually with increase of amplitude of initial motion. This tendency is seen from Fig. 7(b) showing the frequency distribution of $t_P - t_M$ with the magnitude of P initial motion as parameter. Consequently, if the discriminative conditions, in which the filter characteristic is taken into consideration, are defined, it is concluded to be capable to determine the onset time of P first arrival for almost all events ($\geq$90 %) within accuracy of $\pm$0.05 sec.

As for S waves, the onset of SH waves could be determined for 79 of 90 earthquakes from which the onset of P waves was determined, and those of SV waves were also well determined, though with somewhat lower percentage because of the more difficult conditions. The four of 11 events of which the onset of SH waves was not identified, were originated by quarry blasts without SH waves. For two of them, remarkable P later phases were mistaken for S waves. For the other five, the S/P ratio was not so high to exceed the threshold. The histogram of the difference between the onset time, t_{SH}, determined here and the onset time,

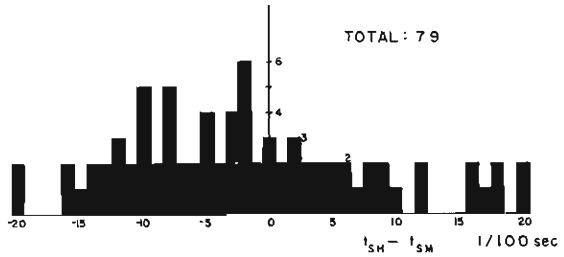

Fig. 8. Histogram of $t_{SH}-t_{SM}$.
t_{SH}: the onset time of SH determined from automated method.
t_{SM}: the onset time of S read visually.

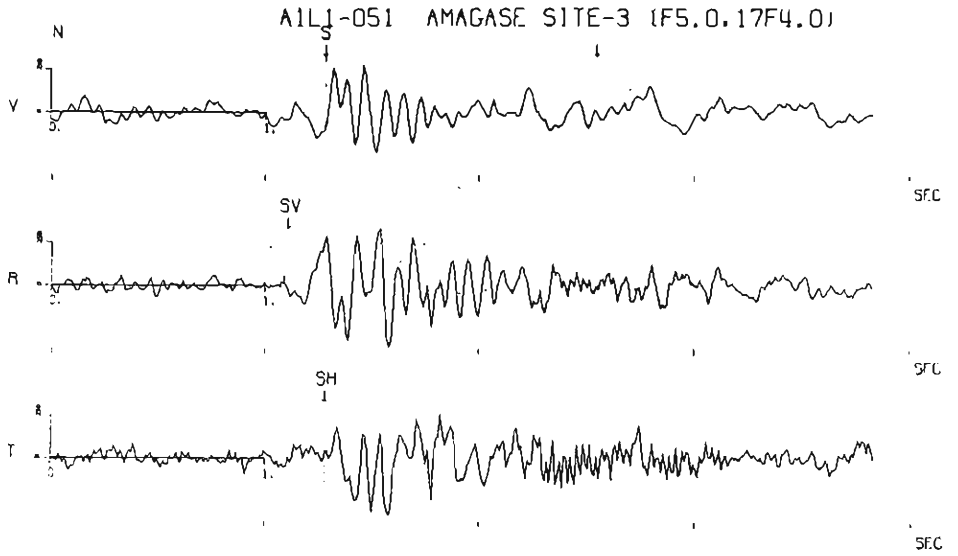

Fig. 9. Waveforms of S wave parts.
Top: vertical component, middle: radial component and down: transverse component. SH means SH onset, SV means SV onset, and S on vertical trace corresponds to SH onset.

t_{SM}, determined by manual reading of seismograms is shown in Fig. 8. As seen from Fig. 8, the distribution of $t_{SH}-t_{SM}$ is fairly uniform within the range of ± 0.20 sec. This is remarkably different from the the case of P. It may be considered that this depends mainly of uncertainty of t_{SM} due to the intrinsic obscurity in reading visually the seismograms, though partly on applying the same threshold over all frequency bands. The waveforms of S portions are shown in Fig. 9 with the onsets of SH and SV by arrows. The mark S on vertical trace represents the onset of SH wave. The example that SV wave of low frequency arrives about 0.2 sec earlier than SH wave is shown in Fig. 9. This is characteristic of earthquakes originated near Kameoka which is situated at the azimuth on N60°W and the S-P time of 3.6 sec from Amagase. On the other hand, there are sometimes such

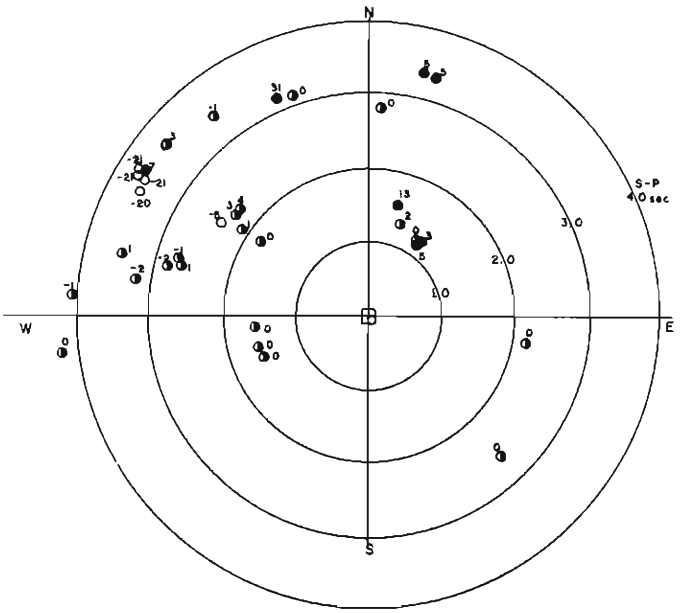

Fig. 10. Locations of epicenters represented by S-P time and azimuth from Amagase. The numbers show the differences between SH onset time and SV onset time: $t_{SV}-t_{SH}$.
●: $t_{SV}-t_{SH}>5/100$ sec, ◑: $|t_{SV}-t_{SH}|<5/100$ sec, and ○: $t_{SV}-t_{SH}<-5/100$ sec.

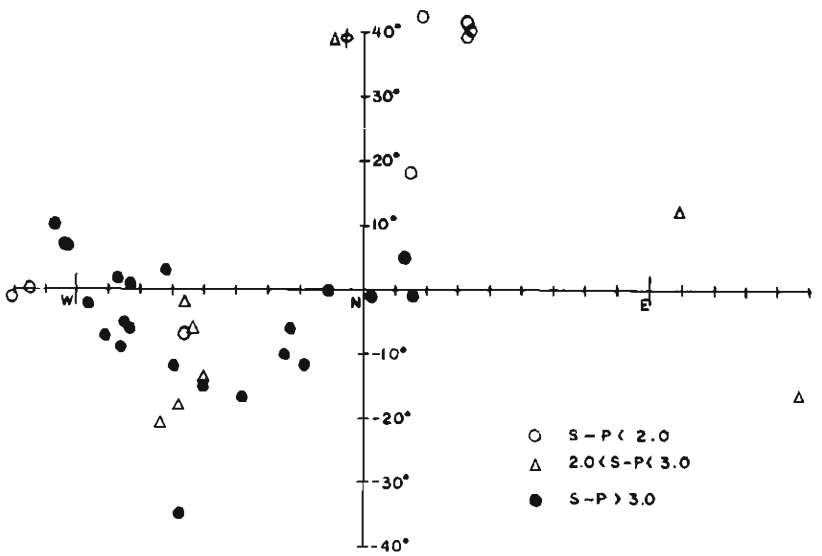

Fig. 11. Deflection of the arrival direction of P wave from the direction of source in the 10~15 Hz band, as a function of azimuth.

cases where SV arrivals are considerably later than SH. For most earthquakes excepting the exceptional cases as described above, there is no evident difference between the onsets of SH and SV. Fig. 10 illustrates the locations of epicenters represented by S-P times and azimuth from Amagase, and the differences of the onset times between SH and SV.

The directions of particle motions of P waves in the horizontal plane show the best agreement with the directions of epicenter in the frequency band of 10~15 Hz. In the higher frequency bands the NS component becomes so significant that the direction tends to deflect to the north-south direction. In the lower frequency bands below 10 Hz, the rectilinearity of particle motion is poor. The comparison between the direction of propagation of P first arrival in the 10~15 Hz band and the direction of epicenter is given in Fig. 11. The result is analogous as obtained previously from the unfiltered records[5], that is, the arrival direction of P wave for the earthquakes with S-P times of 3 to 5 sec deflects to west. But the maximum deflection is found in the northwest direction and the P arrivals from the north direction have no deflection. For the earthquakes with S-P times below 2 sec arriving from the northeast direction, the measured azimuth remarkably deflects to the east. On the other hand, for the quarry blasts near these earthquakes the agreement between the azimuth of P arrival and the azimuth of source is very good. Since these earthquakes are located outside the observational net used for the determination of epicenter, the reliability of source determination is poor. So

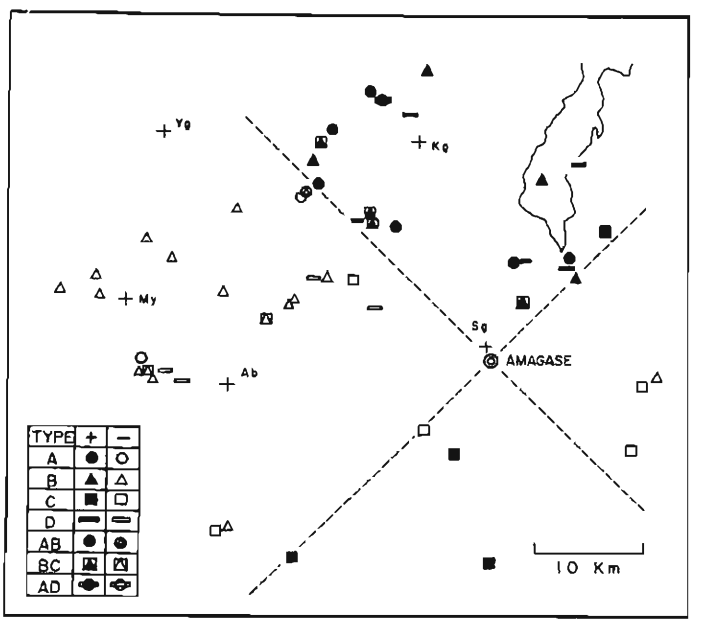

Fig. 12. The regional variation of P wave spectra.
A: the lowest peak frequencies (around 10 Hz), B: relatively higher ones (13 ~16 Hz), C: the highest ones (>20 Hz), D: flat without predominant peak. Closed and open symbols denote push and pull initial motions, respectively.

then it may be considered that this deflection could reflect the inaccuracy of source determination. However, considering that the angle of incidence is strongly different from that of quarry blast, it may reflect some heterogeneity of deep structure.

The nature of spectra of P waves from local earthquakes recorded at Amagase was described in the present author's previous works[4,10]. According to those results, the spectra of P waves are classified generally into four types, A, B, C and D types respectively, based on the predominant frequencies. The events of A type have the lowest peak frequencies (around 10 Hz), those of B type have relatively higher ones (13~16 Hz), and those of C type have the highest ones (>20 Hz). The spectra of D type are almost flat without predominant peaks. The types of spectra above mentioned are plotted at the hypocenters with each symbol in Fig. 12. It is considered that the distribution of the type of spectra depends strongly on the location of source, as seen from Fig. 12. Events of A type occur frequently in the northern region, those of B type in the region between northwest and west and those of C type in the southern region away from the seismic active region. That is, peak frequencies of P spectra for the earthquakes from the seismic active region appear to be lower than those in the region where seismic activity is low. Spectra of S

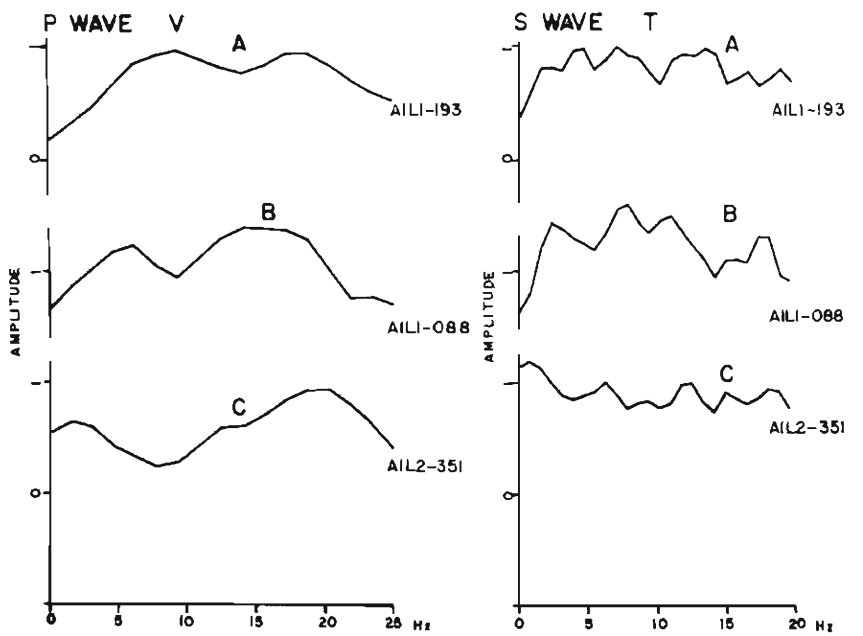

Fig. 13. An example of amplitude spectra of P vertical and SH components from each group of A, B, and C types in Fig. 12.

waves are not classifiable so evidently as those of P. Fig. 13 shows an example of P and S spectra from each group of A, B and C types in Fig. 12. P wave spectra show vertical spectra over window of 0.64 sec from onset and S wave spectra show those of SH component over window of 1.28 sec from onset.

5. Conclusion

The system of automated analysis of local earthquakes (S-P$<$10 sec) obtained from the Amagase short-period seismic observational system has been described. Though the method described here can be applied only to the seismograms recorded at Amagase where the site characteristic is well known, the present result could give a hope to enable us to obtain more accurate determination of seismic parameters than before, by utilizing a suitable system at one observational site. Moreover, considering that the site described here is never thought of as exceptional, in other words, must be thought of as being the usual, the present system may be accepted widely for the usual observatory. For P waves, the onset time with accuracy of 0.1 sec, the azimuth of arrival, the angle of incidence and the duration of the initial motion can be determined by use of this system. As for S waves, the onset time can be determined with accuracy of $\pm$0.2 sec for about 90 % of events of which the onset time of P wave is defined. This accuracy may be improved provided that the reliable onset of S wave is defined evidently by reexamining the nature of S waves. Spectral windows of 0.64 sec for P waves and of 1.28 sec for S waves have been used for convenience of computation. But it is necessary to use the duration time of P or S initial motions for more detailed examination of the nature of the source. A detailed analysis of the preliminary results obtained for P and S waves based on this analytical system is in progress. Furthermore, automated analysis for farther earthquakes with predominant frequency below 10 Hz are intended to be examined.

Acknowledgment

The author wishes to express his sincere thanks to Dr. Tatsuhiko Wada of Kyoto University for much valuable advice and encouragement in carrying out this work, and also to Prof. Michio Takada for his encouragement. The author is indebted to Messrs. Kojiro Irikura and Junpei Akamatsu, his colleagues, for their valuable discussions and co-operation in the preparation of the program for the various computations, and to Mr. Akio Hirono for his help.

The data processing was run on a FACOM 230-25 at the Information Data Processing Center for Disaster Prevention Research of the Disaster Prevention Research Institute of Kyoto University.

References

1) Furuzawa, T.: Some problems of seismic data processing, Part 1, Bull. Disast. Prev. Res. Inst., Kyoto Univ., Vol. 24, 1974, pp. 49-66.
2) Кейлис-Борок, В. И.: Сейсмология и Логика, Вычислительная Сейсмология, Вып. 4, «Наука», 1968, 317-350.
3) Bolt, B. ed.: Methods in computational physics, Vol. 11, 12, Academic Press, 1972.
4) Furuzawa, T., K. Irikura, S. Takemoto and J. Akamatsu: Spectra of body waves from local small earthquakes in the southern parts of Kyoto, Bull. Disas. Prev. Res. Inst., Kyoto Univ., Vol. 22, 1972, pp. 23-36.

5) Furuzawa, T., S. Takemoto, K. Irikura and J. Akamatsu: Local crustal effects on earquake seismograms, Annuals Disas. Prev. Res. Inst., Kyoto Univ., No. 14A, 1971, pp. 189-202.
6) Birtill, J. W. and F. E. Whiteway: The application of phased arrays to the analysis of seismic body waves, Phil. Trans. Roy. Soc., London A, Vol. 258, 1965, pp. 421-493.
7) Wada, T. and T. Kamo: An equipment for a automatically seismic recording, Annuals Disas. Prev. Res. Inst., Kyoto Univ., Vol. 13A, 1970, pp. 35-40.
8) Flinn, E. A.: Signal analysis using rectilinearity and direction of particle motion, Proc. IEEE, Vol. 53, 1965, pp. 1874-1876.
9) Phinny, R. A. and S. W. Smith: Processing of seismic data from an automated digital recorder, Bull. Seism. Soc. Am., Vol. 53, 1963, pp. 549-562.
10) Furuzawa, T., K. Irikura and J. Akamatsu: Regional variation of body waves' spectra from local small earthquakes occuring in the southern parts of Kyoto, Zisin, Vol. 26, 1973, pp. 275-284.